International Journal for Housing Science and Its Applications
Publish August 6, 2025. Volume 46, Issue 3 Pages 5055-5067

https://doi.org/10.70517/ijhsa463433

Noise source control and design of Fe-based soft magnetic composite core reactor based on optimization algorithm

Yangyang Ma[1], Wenle Song[1], Jie Gao[2,*], Yang Liu[2], Yilei Shang[2], Weimei Zhao[2] and Fuyao Yang[2]
[1] State Grid Cangzhou Electric Power Supply Company, Cangzhou, Hebei, 061000, China
[2] China Electric Power Research Institute, Beijing, 100192, China
Corresponding authors: (e-mail: conch3501@163.com).

Abstract As a key equipment in the power system, the noise problem of dry-type iron core reactor directly affects the stability of equipment operation and the user's environmental experience. Based on the multi-physical field coupling theory, this study analyzes the vibration noise formation mechanism and optimization control method of Fe-based soft magnetic composite core reactor by combining COMSOL simulation and experimental test. The contributions of Maxwell force and magnetostrictive effect to the vibration of the core are quantified by coupled electromagnetic-mechanical-acoustic field modeling. The results show that the maximum vibration displacement induced by Maxwell force is 3.81×10^{-5} m, which is much higher than that of magnetostrictive force of 3.56×10^{-8} m. Aiming at the insensitivity of air-gap structural parameter, the topology optimization algorithm of electromagnetic-mechanical-acoustic field coupling is proposed, which reduces the vibration displacement of the Fe-based soft magnetic reactor by 90.19% from 9.41×10^{-7} m to 9.23×10^{-8} m. After the optimization, the vibration noise formation and control method of the Fe-based soft magnetic reactor are optimized. The optimized Fe-based soft magnetic reactor has a high voltage noise of 45.71 dB(A) and a sound power value of 58.93 dB(A), which are 31.9% and 28.7% lower than that of the conventional silicon steel reactor, respectively.

Index Terms dry core reactor, Fe-based soft magnetic composite, COMSOL, electromagnetic-mechanical-acoustic field coupling, air gap structure

I. Introduction

With the increase in power loads as well as the complexity of power systems, the demand for reactors is also increasing and they have become an integral part of power systems [1]. Reactors play a role in power systems to regulate voltage, improve system stability and enhance power quality. Reactors can be classified into iron core reactors and hollow core reactors according to their structure, which are widely used for reactive power compensation, harmonic suppression, short-circuit current limitation, and system voltage stabilization [2], [3].

In today's power systems, ferrocentric reactors and hollow reactors play their respective advantages in different scenarios. Hollow-core reactors are larger in size, have lower environmental requirements, are suitable for outdoor environments, and are commonly used in high-voltage power systems, such as substations and transmission lines [4], [5]. However, the magnetic field generated by it has a wide range of influence and is prone to electromagnetic pollution, which adversely affects the surrounding electrical equipment and systems [6]. The core reactor is smaller compared to the hollow reactor and is widely used in low-voltage power systems, especially in the voltage level of 10 kV, which is used in large quantities [7]-[9]. However, with the long-term operation of reactors, partial discharges and noise problems inside the device will lead to continuous deterioration of insulation [10].

The noise of the reactor is an extremely important technical parameter to measure the performance index of the reactor [11]. The level of reactor noise is also naturally one of the important indicators of the design capability and manufacturing level of reactor manufacturers [12], [13]. Therefore, many reactor manufacturers are actively taking various measures as a way to reduce reactor noise. The noise sources of the core reactor can be divided into two kinds, i.e., the body noise and the noise of the cooling system [14]. Among them, the intrinsic noise is inherent in the reactor itself, including electromagnetic vibration and winding vibration [15]. Electromagnetic suction is one of the critical factors leading to electromagnetic vibration of the reactor. Electromagnetic suction, which is Maxwell's force, is due to the fact that when the main magnetic flux passes through the core with high permeability and the air gap with low permeability, some kind of force that makes the magnetic field energy smaller forces the reactor core to undergo periodic deformation [16], [17]. Yan, R et al. in their study of Maxwell's force solved the problem of reactor vibration and noise by finding out that by accessing a core reactor in an AC circuit, the finite element model calculates the stresses in the gapped core reactor and by analyzing the stress distributions and spectra of the

reactor under various excitation conditions [18]. Zhang, P et al. simulated and experimentally verified the core vibration in a reactor and explored the effect of air gap on the vibration noise of the reactor core and the roles of Maxwell stress and magnetostriction in triggering the vibration process [19]. Rossi, M and Le Besnerais, J studied the case of vibration noise in reactors due to Maxwell's force and magnetostrictive force and proposed a method to reduce the vibration noise by canceling these forces [20]. Magnetostriction has a complex nonlinear relationship, and the establishment of magnetostrictive forces describing the phenomenon of magnetostriction is the basis for the calculation of electromagnetic vibration in core reactors [21].

In order to effectively reduce the vibration noise of the core reactor, scholars at home and abroad have made a lot of efforts, and the main starting points of the research on vibration and noise reduction problems are different. For example, Loizos, G et al. investigated the local magnetic field situation distribution of Si-Fe distributed gap cores, and proposed a method to increase the external preload to reduce the magnetic force in the lap region so as to reduce the contribution of magnetostriction to vibration [22]. Wang, Z et al. in their study analyzed the vibration characteristics of series core reactors and achieved an average 11.6% magnitude reduction in vibration noise through a specific damping scheme, which in turn enhanced the performance and safety of the core reactors [23]. Zhu, S et al. optimized the design parameters of an oil-immersed core reactor using particle swarm optimization and thermal network model, which achieved a 23.05% reduction in metal conductor usage and a 20.25% reduction in losses by taking metal conductor usage and winding losses as optimization targets [24]. Gao, L et al. studied the vibration and noise characteristics of air-core reactors in a high-voltage DC converter station, and analyzed the generation process, intrinsic frequency, and noise distribution as a basis for noise control [25]. Adıbek, T et al. used an improved noise reduction design scheme to reduce and eliminate vibration and noise in shunt oil reactors, thereby mitigating their environmental impact, significantly reducing the background noise level, and effectively extending the service life of the reactors [26]. Gao, Y et al. built a model of the reactor and made a more detailed analysis of its magnetic field calculation, analyzed some of the nodal forces for the brief model of the reactor, in which the magnetostrictive forces were calculated using equivalent nodes, and proposed the effect of the high-hardness air-gap dielectric material on the vibrational forces at the nodes [27]. Tong, B et al. investigated the stress characteristics in magnetically controlled saturable reactors (MCSRs) with the aim of developing new methods for vibration and noise reduction by proposing an electro-mechanical model to analyze the vibrations caused by magnetostrictive and electromagnetic forces [28]. Moses, A. J et al. reduced transformer core vibration and noise by bonding technique, and then analyzed the relationship between transformer core vibration and noise [29]. At present, the vibration research and noise suppression of core reactors are still in the beginning stage, while magnetostriction is the key to cause vibration and noise problems, and the special structure of the core reactor makes the complexity of the magnetostriction characteristics of Fe matrix composites [30], [31]. Therefore, further in-depth studies are still needed to consider the effect of core preload on the vibration of the reactor and how to suppress the vibration of the reactor.

In order to deeply investigate the formation mechanism of the noise source and optimize the design, this study starts from the structural characteristics of the core reactor and combines the multi-physical field theory analysis method. The coupling mechanism of electromagnetic-mechanical-acoustic field is systematically investigated, and theoretical modeling is carried out for the influence of uncertainty of air gap structure parameters on vibration noise. The article first elaborates the basic structure and key parameters of dry-type iron core reactor. Through the simplified model construction, it is clarified that the core is made of cold-rolled oriented silicon steel sheets laminated together, the air gap is separated by epoxy-laminated glass cloth panels, and the coil adopts a multilayer cartridge winding structure. On this basis focuses on the theoretical analysis of multi-physics field coupling. The structural force field model is established by COMSOL solid mechanics module, focusing on the contribution of magnetostrictive effect and Maxwell force to the core vibration. Based on the linear elasticity equation, the mathematical relationship between magnetostrictive strain and stress tensor is derived, and the small effect of the magnetostrictive coefficient of silicon steel sheet on core deformation is quantified. Meanwhile, the distribution characteristics of electromagnetic force in the core and winding are clarified by combining Maxwell's force equation and Lorentz force model. And turning to the acoustic field analysis, the transfer path of core vibration to noise radiation is established by solving the acoustic pressure fluctuation equation and the acoustic pressure-velocity relationship through the pressure acoustic field module. The mechanism of the influence of the uncertainty of the air gap structure parameters on the core vibration is further explored. By analyzing the sensitivity of the Maxwell stress tensor and the effectiveness of magnetostriction, it is revealed how the variation of the air gap dimensions leads to the fluctuation of the magnetic flux density and the magnetic field strength, which in turn triggers the uncertainty of the magnitude and distribution of the electromagnetic force. Combined with the vibration equations, the transmission mechanism of parameter uncertainty on core vibration displacement is clarified. And the chain effect of air gap parameter variation on vibration noise is systematically summarized.

II. MSCR-based analysis of vibration and noise mechanism and the influence of air gap parameters in core reactor

II. A.Basic structure and parameters of dry-type core reactor

The research object of this paper is a single-phase dry-type core reactor with a rated voltage of 10 kV and a frequency of 50 Hz, and a simplified model is made in order to take into account the calculation accuracy and calculation efficiency.

Dry-type core reactor core part consists of cold-rolled oriented silicon steel sheet, the core column of each pancake is evenly divided by a number of air gaps between the air gaps using epoxy laminated glass cloth plate as a spacer. The coil part is wound by multi-layer cylinder structure, and the wire inside the coil is flat copper wire wrapped with insulating layer, the number of layers is 3 layers, and the layers are fixedly connected with each other by bracing strips to form axial heat dissipation airway between the coils. The core is fixed externally by clamps and tie rods, and the core lamination factor is 0.97. The main structural parameters of the core reactor are shown in Table 1.

Table1: Structural parameters of the core reactor

Structure	Parameters	Value
Iron heart	Core diameter /mm	300
	Yoke height /mm	145
	The height of the discus /mm	45
	Total height of air gap /mm	88
	Air gap number	7
	Cross-sectional area of the core column /cm²	545
Coil	Inner coil width /mm	18
	Middle coil width /mm	27
	Outer coil width /mm	27
	Coil height /mm	475
	Cross-sectional area of the wire /mm²	8.52

II. B.MSCR multiphysics field theory analysis

Based on the above structural characteristics and parameters of the core reactor, its vibration and noise generation is essentially a result of the coupling of electromagnetic, mechanical and acoustic multiphysics fields. Therefore, in this section, the quantitative analysis model of core vibration and noise radiation is established from the dimensions of structural force field and acoustic field, respectively, in combination with the MSCR multiphysics field theory.

II. B. 1) Structural force field analysis

In the structural force field simulation, the solid mechanics module in COMSOL is selected, and the structural force field solution domain equations are shown in the following equation:

$$m\frac{d^2u}{dt^2}+\zeta\frac{du}{dt}+ku=F_v \tag{1}$$

where m is the mass matrix; ζ is the damping coefficient matrix; k is the stiffness matrix; and u is the displacement vector.

In order to describe the mechanical equations of the core, the linear elasticity equation is chosen to describe the magnetostriction:

$$\nabla\cdot\sigma=-F_v \tag{2}$$

where σ is the stress tensor in N/m and F_v is the volumetric force in N/m³.

The so-called magnetostriction is a phenomenon in which the size of a magnetic material changes in all directions due to a change in the magnetization state of the magnetic material under the action of an applied magnetic field. When the applied magnetic field is removed, the ferromagnetic material will return to its original shape. The magnetostriction effect of ferromagnetic materials can be divided into two categories, one is line magnetostriction and the other is body magnetostriction. Linear magnetostriction is a change in the length of a ferromagnetic material under the action of an applied magnetic field, where the length of the material is elongated or shortened. Body magnetostriction is a change in the volume of a ferromagnetic material under the action of an applied magnetic field. Under the action of an applied magnetic field, line magnetostriction and body magnetostriction will exist at the same

time, but the strength of the magnetic field is different at the same time, the two kinds of magnetostriction produced by the impact of the role of the different, if one effect is the main effect, then the other is a secondary effect.

The magnetization process of the ferromagnetic material is the main influence of the line magnetostriction effect, while the body magnetostriction effect occurs when the magnetic field strength is greater than the saturation field strength, when the internal magnetization strength of the material is greater than the spontaneous magnetization strength. Since in ferromagnetic materials, the spontaneous magnetization strength is related to the exchange between its spins, the nature of the force generated by the body magnetostriction effect is an exchange force. Since bulk magnetostriction occurs mainly as an increase or decrease in the volume of the material, it predominates when the ferromagnetic material reaches saturation.

At present, the magnetostriction effect is dominated by three forms of magnetostriction along the magnetic field direction, magnetostriction along the perpendicular direction of the magnetic field, and volume change magnetostriction of magnetic materials. Among them, the magnetostriction effect of volume change is very small, so scholars can ignore the influence of this factor when carrying out related research. Therefore, this paper only considers the transverse magnetostriction along the direction of the magnetic field and the longitudinal magnetostriction along the direction of the perpendicular magnetic field, both of which belong to the linear magnetostriction. Due to the complexity of the intrinsic relationship of magnetostriction effect, so far there is no canonical unity conclusion related to it, so usually according to experience, the transverse magnetostriction and longitudinal magnetostriction change with the nature of the material Poisson's ratio analogous to analyze and study, that is, the magnitude of the magnetostriction effect and the magnitude of the applied magnetic field and the ferromagnetic material's own properties of the relationship is close.

Since the amount of change in the length of the ferromagnetic material caused by the linear magnetostrictive effect is small, the magnitude of magnetostriction is described by the relative change in length, as shown in the following equation:

$$\lambda = (L_H - L_0) / L_0 \tag{3}$$

where L_0 is the initial length of the magnetic material; L_H is the length of the ferromagnetic material after elongation or shortening under the action of an applied magnetic field.

The coefficient of magnetostriction of the electrical silicon steel sheet used in MSCR is about one part per million, usually expressed in ppm. The linear magnetostrictive effect of ferromagnetic materials is reflected at the microscopic level by changes in the magnetic domains within ferromagnetic materials including iron, nickel, cobalt, and their alloys.

When the ferromagnetic material is located in the magnetic field, the magnetic field within the material will change, after stabilization will be a significant enhancement of the potential, which makes the ferromagnetic material in the external magnetic field presents a strong magnetic, this phenomenon is known as the ferromagnetic material magnetization. This phenomenon is called the magnetization of ferromagnetic materials. Ferromagnetic materials can be magnetized because there are many very small natural magnetization zones called magnetic domains, and each magnetic domain can be regarded as a miniature magnet. When an external magnetic field is applied to a ferromagnetic material, the direction of its magnetization changes, and when stabilized, the internal magnetic domains are in the same direction as the magnetic field. The process of magnetic domain change is macroscopically manifested as a change in the length and width of the ferromagnetic material, and the change in the size of the ferromagnetic material due to the change in rotation of the internal magnetic domains is shown in Figure 1.

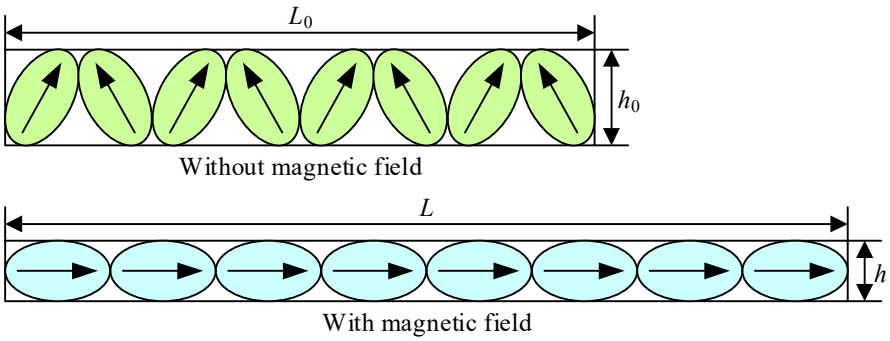

Figure 1: Magnetic domain state transformation

In this paper, the following magnetostriction model is used for the calculation: the calculation of magnetostriction is defined as a function of the initial strain loaded into the reactor core, which serves as the excitation source for the magnetostriction of the core. Where the magnetostriction can be viewed as a function of the magnetization along any direction and is expressed by the following equation:

$$\lambda_i = \frac{3}{2}\lambda_s\left(\alpha_i^2 - \frac{1}{3}\right) = \frac{3}{2}\lambda_s\left\{\left(\frac{M_i}{M_s}\right)^2 - \frac{1}{3}\right\} \tag{4}$$

where, the magnetostriction λ_i along the i-direction depends on the magnetostriction constant λ_s and the directional cosine of the magnetization strength α_i, where the directional cosine is the ratio of the material's magnetization strength along the i-direction to the saturation magnetization strength. -1/3 means that the magnetic domains are random in the absence of any magnetic field, and the term can be omitted because all the magnetic dipole moments and the magnetization direction are perpendicular to the magnetization direction at the beginning of the magnetization process of the actual core material. So the above equation can be simplified as:

$$\lambda_i = \frac{3}{2}\lambda_s\alpha_i^2 = \frac{3}{2}\lambda_s\left(\frac{M_i}{M_s}\right)^2 \tag{5}$$

Core reactors generally have an air gap, and neighboring core cakes are adjacent to each other at any instant of time with heteromorphic poles, so the Maxwell force between them is an attractive force, and the magnitude of the Maxwell force is:

$$F = \frac{B^2 S}{2\mu_0} = \frac{\Phi^2}{2\mu_0 S} \tag{6}$$

where F is the Maxwell force; μ_0 is the vacuum permeability; B is the magnetic induction in the air gap; S is the flux area; and Φ is the flux.

In the case of industrial frequency:

$$\Phi = \Phi_m \sin \omega t \tag{7}$$

Therefore, the above equation can be reduced to:

$$F = \frac{\Phi^2}{2\mu_0 S} = \frac{\Phi_m^2}{2\mu_0 S}\sin^2 \omega t \tag{8}$$

Let $F_m = \frac{\Phi_m^2}{2\mu_0 S}$, then the Maxwell force reduces to:

$$F = \frac{F_m}{2}\left(1 - \cos 2\omega t\right) \tag{9}$$

The Lorentz force on the windings is loaded into the reactor windings as a body load and the Lorentz force on the windings is given by the following equation:

$$F = J \times B \tag{10}$$

where J is the current density in A/m² and B is the magnetic flux density in T.

II. B. 2) Sound field analysis

The pressure sound field module is selected in the sound field analysis, and the variable solved for in the pressure sound field module is the sound pressure p. The solved domain sound pressure fluctuation equation is:

$$-\frac{1}{c^2}\frac{\partial^2 p}{\partial t^2} + \nabla^2 p = 0 \tag{11}$$

where c is the speed of sound in m/s² and p is the sound pressure in Pa.

The relationship between sound pressure and sound velocity can be described by applying the linear equation of motion as:

$$\rho_0 \frac{\partial u}{\partial t} = -\nabla p \tag{12}$$

where ρ_0 is the air density in kg/m³.

II. C. Theoretical analysis of reactor core vibration under uncertainty of air gap structure parameters

Multi-physical field coupling analysis lays the foundation for the mechanism study of core vibration noise, but the manufacturing tolerance of air gap structural parameters and service aging in actual engineering may cause the theoretical model to deviate from the actual working conditions. Therefore, this section will focus on the dynamic effects of the uncertainty of the air gap parameters on the electromagnetic force distribution and vibration response to improve the engineering applicability of the theoretical model.

The vibration of the shunt reactor core is caused by the electromagnetic force on the core, and under the action of the magnetic field, the electromagnetic force F_v on the core is the vector sum of the Maxwell's force $F_{\max}$ and the magnetostrictive equivalent force F_{ms}, i.e.

$$F_v = F_{\max} + F_{ms} \tag{13}$$

where Maxwell's force $F_{\max}$ acts at the interface between the air gap and the core cake on the core column, calculated as

$$F_{\max} = \oint_S T dS \tag{14}$$

where S is a closed surface enclosing a portion of the core material; T is the Maxwell stress tensor, which is a second-order tensor computed as

$$T = \begin{bmatrix} B_x H_x - \frac{1}{2} BH & B_x H_y \\ B_y H_x & B_y H_y - \frac{1}{2} BH \end{bmatrix} \begin{bmatrix} n_x \\ n_y \end{bmatrix} \tag{15}$$

where B is the magnetic flux density of the reactor core; B_x and B_y are the components of the magnetic flux density in the x-axis and y-axis directions; H is the magnetic field strength of the reactor core; H_x and H_y are the components of the magnetic field strength in the x-axis and y-axis directions; and n_x and n_y are the components of the unit normal vector in the x and y direction components. Uncertainty changes in the parameters of the air-gap structure cause uncertainty changes in the magnetic flux density B and magnetic field strength H inside the core, which can be seen in Eqs. (14) and (15), and changes in the magnetic flux density and magnetic field strength lead to changes in the Maxwell stress tensor, which in turn cause uncertainty changes in the Maxwell force.

The magnetostrictive equivalent force F_{ms} is derived from the magnetostrictive strain equivalent of ferromagnetic materials, and the relationship between the magnetostrictive stress tensor and the magnetostrictive equivalent force for linearly elastic materials in structural mechanics is

$$F_{ms} = \nabla \cdot \sigma \tag{16}$$

where ∇ is the gradient operator; σ is the magnetostrictive stress tensor of the core, calculated as

$$\sigma = D\varepsilon \tag{17}$$

where D is the elasticity tensor matrix; ε is the magnetostrictive strain, which can usually be obtained from the magnetic field strength H in the core by the magnetostrictive orthogonal interpolation method ε. The elastic tensor matrix D has the form

$$D = \frac{E(1-\alpha)}{(1+\alpha)(1-2\alpha)} \begin{bmatrix} 1 & \frac{\alpha}{1-\alpha} & \frac{\alpha}{1-\alpha} \\ \frac{\alpha}{1-\alpha} & 1 & \frac{\alpha}{1-\alpha} \\ \frac{\alpha}{1-\alpha} & \frac{\alpha}{1-\alpha} & 1 \end{bmatrix} \tag{18}$$

where E is the Young's modulus of the core; α is the Poisson's ratio.

Uncertainty changes in the parameters of the air-gap structure cause uncertainty changes in the magnetic field strength H inside the core, making the magnetostrictive strain ε, which is highly correlated with the magnetic field strength H, change. On this basis, it can be seen from Eq. (16) and Eq. (17) that the change of magnetostrictive strain ε leads to the change of magnetostrictive stress tensor, which in turn causes the change of uncertainty in the effectiveness of magnetostrictive equivalence. In summary, it can be seen that uncertainty variations in the parameters of the air gap structure lead to uncertainty variations in the values of the Maxwell force and the magnetostriction equivalence force, which in turn cause uncertainty variations in the magnitude of the electromagnetic force applied to the core, which consists of the two together.

In addition, in terms of the distribution of the electromagnetic force on the core, due to the large difference in permeability between the core cake and the air gap on the core column, the core cake being a high permeability silicon steel material while the air gap is a low permeability marble material, the magnetic flux generates a Maxwell stress tensor as it passes through the interface between the air gap and the core cake. As the Maxwell force acts at the interface between the core cake and the air gap, uncertainty variations in the air gap structural parameters change the position of the core cake and the air gap boundary, thus changing the distribution of the Maxwell force; for the magnetostriction equivalent force, which is derived from the equivalent of the magnetostriction phenomenon in ferromagnetic materials, acting on the iron yoke and the core cake, and uncertainty variations in the air gap structural parameters change the position of the core column on the iron core cake position on the core column, thus changing the distribution of the magnetostrictive equivalent effect. Therefore, uncertainty variations in the air gap structure parameters also change the distribution of electromagnetic forces in the core.

The components of the reactor core are all linear elastic materials, ignoring the damping effect, the vibration displacement size of the core can be found by the vibration equation in structural mechanics, namely

$$M_c a + K_c u = F_v \tag{19}$$

where M_c is the mass matrix of the core; K_c is the stiffness matrix of the core, u is the vibration displacement of the core; and a is the vibration acceleration of the core. From Eq. (19), it can be seen that the uncertainty variation of the air gap structure parameters changes the distribution of vibration sites and the magnitude of vibration values of the reactor core by affecting the magnitude and distribution of the electromagnetic force applied to the core. The flow of the effect of uncertainty variation of air gap structure parameters on vibration is shown in Fig. 2.

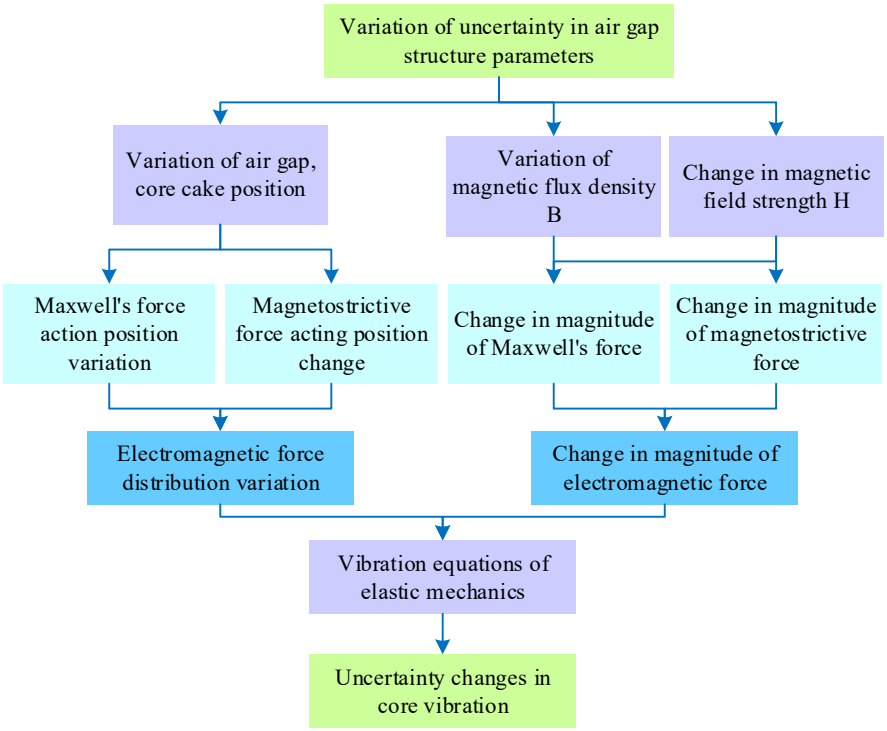

Figure 2: The impact of uncertain changes in gap structural parameters on vibration

III. Vibration and noise simulation of Fe-based soft magnetic composite reactor based on optimization algorithm

Based on the quantitative analysis of the formation mechanism of core vibration noise under the uncertainty of air gap parameters in Chapter 2, this chapter will combine the multiphysics field simulation and experimental test to explore the specific application of optimization algorithm in the vibration and noise reduction design of Fe-based soft magnetic composite reactor and verify its effect in engineering practice.

The simulation calculation can truly reflect the operation of the simulation object. At the same time, the simulation calculation can reduce the cost of engineering cost, eliminate or reduce the potential problems existing in the engineering design, help the product development and improvement, further improve the performance and reliability of the product, and provide a more correct and reliable theoretical analysis for the design program. In order to analyze the effects of Maxwell force and magnetostrictive force on reactor vibration in more detail, and on this basis to reveal the vibration characteristics of the core of series reactor under normal operation, it is necessary to carry out a simulation study on the vibration of the reactor under fundamental and harmonic conditions.

III. A. Simulation Parameter Settings

In order to verify the noise reduction effect of Fe-based soft magnetic composites, simulation modeling and analysis of silicon steel series reactor and Fe-based soft magnetic series reactor with model number CKSC-300/10-5 are carried out in this paper. Both reactors have a rated operating current of 320 A. The outer dimensions of the Fe-based soft magnetic reactor core are 1073 mm × 1387 mm × 238 mm, and the core window dimensions are 1036 mm × 186 mm, containing four 5-mm air gaps per phase. The outer dimensions of the silicon steel reactor core are 871mm×1502mm×180mm, the core window size is 1091mm×180mm, and each phase contains six 5mm air gaps. Meanwhile, when the vibration displacement is calculated in the simulation, fixed constraints are added to the bottom and top of the series reactor, i.e., the displacement magnitude is 0. This is used to simulate the standing operation of the reactor and the constrained state of the top fasteners. The simulation parameters of the series reactor are as follows: Young's modulus E of both silicon steel and Fe-based soft magnetic composites is 0.35 GPa, the number of turns N of the excitation coils of both are 118 and 42, the effective cross-sectional areas S of the core columns are 0.0317 and 0.0498 m², and the core ρ is 7671 and 8154 kg/m², respectively.

III. B. Numerical simulation of core vibration of series reactor

This section quantifies the contribution of magnetostriction and Maxwell's force to the vibration displacement by comparing the vibration characteristics of silicon steel and Fe-based soft magnetic composite reactors through numerical simulations.

III. B. 1) Series reactor core simulation results

Since Fe-based soft magnetic composites do not have low magnetostrictive properties like silicon steel materials, in order to investigate the contribution of magnetostrictive and Maxwell forces to the vibration displacements, this paper compares the maximum vibration displacements generated by Maxwell and magnetostrictive forces, respectively, in Fe-based soft magnetic composite reactors under the fundamental wave condition, and the results are shown in Fig. 3.

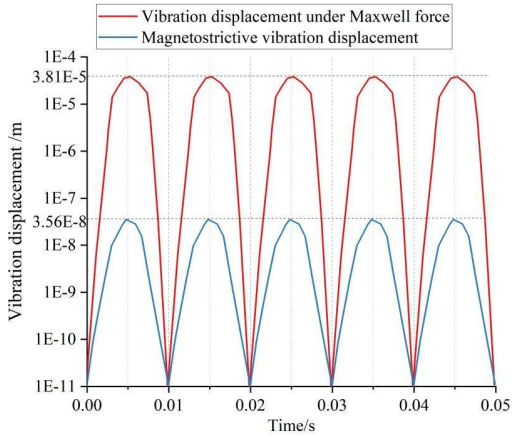

Figure 3: Comparison of Maxwell and magnetostrictive on vibration displacement

From Figure 3 can be seen that the magnetostrictive force caused by the reactor core vibration displacement is much smaller than the Maxwell force caused by the reactor core vibration displacement, Maxwell force generated by the maximum vibration displacement of 3.81 × 10^{-5}m, while the magnetostrictive force generated by the maximum vibration displacement is only 3.56 × 10^{-8}m.

In the power system, the operation of electrical equipment will generate high harmonics such as 3, 5, 7, 9, 11, etc., and the shunt capacitor series reactor is applied in the project to carry out harmonic management, so the series reactor works in the working condition containing a large number of harmonics. In this paper, the harmonic excitation is superimposed on the basis of the fundamental wave to obtain three symmetrical harmonic currents, mainly on the fundamental wave +60% of the harmonic conditions of the vibration displacement caused by Maxwell force for time-frequency analysis, harmonic conditions of Fe-based soft magnetic series reactor Maxwell force caused by the vibration displacement of the spectral analysis of the vibration is shown in Figure 4.

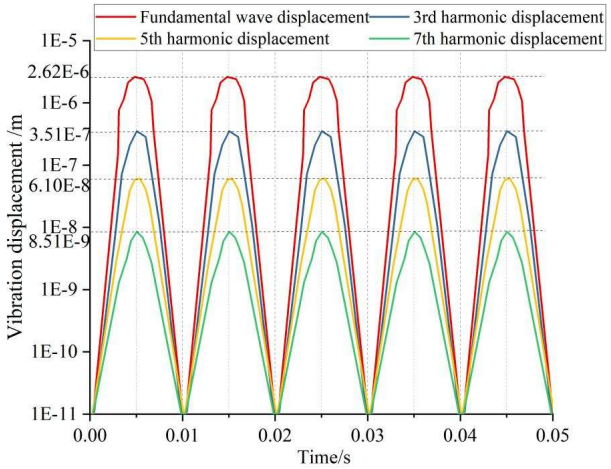

Figure 4: Analysis of vibration displacement by Maxwell under harmonic conditions

When the harmonic content is 60%, the maximum vibration displacement of the original fundamental wave is 2.62×10^{-6}m, the third harmonic will have some effect on the vibration displacement, which will slightly reduce the vibration displacement of the reactor and make the maximum vibration displacement decrease to 3.51×10^{-7}m, and the vibration displacement caused by the fifth and seventh harmonics is much smaller than that caused by the fundamental wave, which are respectively 6.10×10^{-8}m and 8.51×10^{-9}m, respectively.

III. B. 2) Comparison of simulation results of core vibration displacement of series reactor

From the analysis in the previous section, it can be seen that harmonics have a small effect on the vibration displacement of the series reactor, and the contribution of magnetostrictive force to the vibration displacement of the reactor is much smaller than the contribution of Maxwell force to the vibration displacement of the reactor core. Therefore, the vibration displacement caused by Maxwell force under the fundamental wave condition can be used to characterize the vibration displacement of the series reactor. A comparison of the vibration displacements of the silicon steel reactor core and the Fe-based soft magnetic composite reactor core measurement points is shown in Fig. 5.

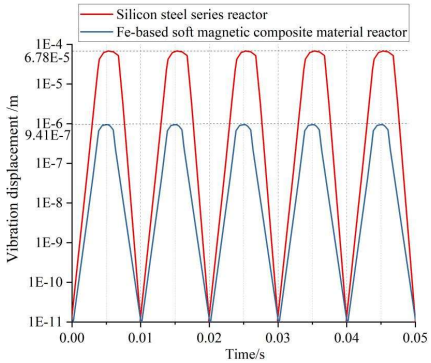

Figure 5: Reactor core measurement point vibration displacement comparison

As can be seen from Fig. 5, the vibration displacement of the Fe-based soft magnetic reactor core is much smaller than that of the conventional silicon steel reactor core. The maximum displacement of the silicon steel series reactor is 6.68×10^{-5}m, while the maximum displacement of the Fe-based soft magnetic series reactor is 9.41×10^{-7}m. Compared with the two, the vibration displacement of the measurement point of the Fe-based soft magnetic composite material series reactor core is 98.61% lower than that of the measurement point of the silicon steel reactor core. It is proved that the Fe-based soft magnetic composites can greatly reduce the vibration displacement of the core surface during the operation of the series reactor.

III. C. Topological simulation analysis of damping structure for Fe-based soft magnetic reactor core

In order to further improve the vibration damping performance of Fe-based soft magnetic reactors, this section introduces the electromagnetic-mechanical-acoustic field coupling topology optimization method to analyze the vibration displacement suppression effect of the damping structure.

III. C. 1) Model convergence analysis

Based on the electromagnetic-mechanical coupled topology optimization model of the reactor and the objective function and constraints, the model simulation solution is carried out, firstly, the analysis of the convergence of the topology optimization using the structural force field model based on the COMSOL Solid Mechanics Module is conducted to compare with the electromagnetic-mechanical-acoustic coupled topology optimization, and the convergence analysis of the electromagnetic-mechanical-acoustic coupled topology optimization model is shown in Fig. 6, in which the traditional topology optimization is the one which takes the 0 as the initial value of the multi-coupling topology optimization, i.e., the initial value of the design variable ρ is zero.

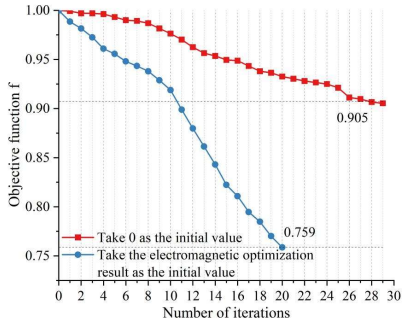

Figure 6: Convergence analysis of Coupled Topology Optimization Model

As can be seen in Fig. 6, the number of iterations of the traditional topology optimization with 0 as the initial value is 29, and the objective function value is 0.905, and the number of iterations of the electromagnetic-mechanical-acoustic field coupled topology optimization with the electromagnetic topology optimization result as the initial value is 20, which is a reduction of 9 times, and at the same time, the objective function value is lowered to 0.759, which is reduced by 16.13%, which indicates that the electromagnetic-mechanical-acoustic field coupled topology optimization possesses higher computational efficiency and better optimization effect.

III. C. 2) Analysis of vibration reduction effect

See Figure 7, the maximum vibration displacement of the Fe-based soft magnetic composite reactor before optimization is 9.41×10-7m, and the maximum vibration displacement is 9.23×10-8m after the optimization of the electromagnetic-mechanical-acoustic field coupling topology optimization with the electromagnetic topology optimization result as the initial value, and the maximum vibration displacement is reduced by 90.19% after optimization. As a result, the topology optimization method of electromagnetic-mechanical-acoustic field coupling of the reactor proposed in this paper has a better vibration damping effect under the premise of ensuring the normal operating condition of the reactor.

III. C. 3) Model Accuracy Verification

In order to verify the accuracy of the simulation model, vibration tests were conducted on the Fe-based soft magnetic composite reactor before and after optimization, and the vibration acceleration in the direction of the main magnetic circuit of the reactor core (i.e., x-direction) was selected for comparison, and the port voltage and current waveforms of the excitation winding are shown in Fig. 8.

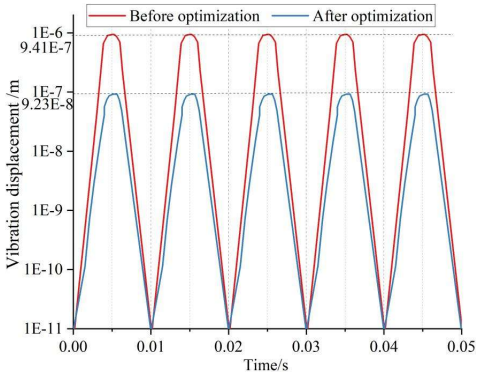

Figure 7: The vibration displacement curve at point P

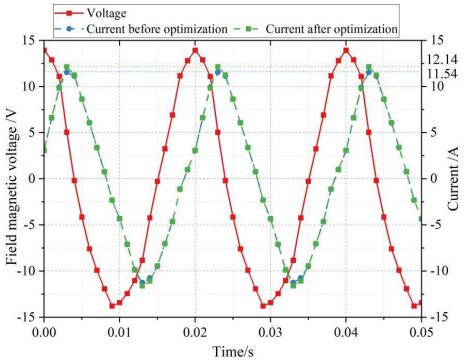

Figure 8: The voltage and current waveforms of reactor

As can be seen from Fig. 8, under the same excitation voltage, the amplitude of the core induced current before and after optimization is 11.54 A and 12.14 A, respectively, and the waveform is basically unchanged; at the same time, the inductance value of the reactor before and after optimization is 4.22 mH and 4.01 mH, respectively, and the value of the inductance is reduced by 4.98% after optimization. The main reason is that due to the structural differences in the core air gap region before and after optimization, the air gap of the reactor after optimization is slightly larger, i.e., the magnetoresistance of the reactor after optimization is larger, resulting in a reduction of the inductance value.

III. D. Noise testing

On the basis of completing the vibration simulation optimization, this section verifies the actual noise reduction capability of the theoretical model and the optimization scheme through noise test experiments, and makes a side-by-side comparison with the traditional reactor.

Noise test of reactor samples is carried out according to the Fe-based soft magnetic composite reactor after electromagnetic-mechanical-acoustic field coupling topology optimization designed in this paper with the electromagnetic topology optimization result as the initial value, and at the same time, comparative experiments are carried out with the pre-optimized Fe-based soft magnetic composite reactor, ordinary silicon steel core reactor and magnetic powder core iron core reactor. The rated voltage is applied to the reactor, the distance of the contour line from the reference plane is 2.0 m, the spacing of the measurement points is 0.9~1 m, and the arrangement of the measurement points is 18, and the height of the measurement points is 0.5 m. The data of the noise test are shown in Table 2.

The measured high-voltage noise value of the silicon steel core reactor is 67.18 dB(A), and the sound power value is 82.68 dB(A), which is the highest noise level among the four types of reactors; the noise performance of the magnetic powder core reactor is the next highest, with the measured high-voltage and sound power values of 50.47 dB(A) and 65.25 dB(A), respectively. In contrast, the noise of the reactor with Fe-based soft magnetic composites is significantly reduced: the measured high voltage value of the Fe-based soft magnetic reactor before optimization is 47.42 dB(A) and the sound power value is 62.31 dB(A); The optimized Fe-based soft magnetic reactor further reduces the high-voltage noise and sound power values to 45.71 dB(A) and 58.93 dB(A), respectively, which are 3.6% and 5.4% lower than the pre-optimization values. Compared with the silicon steel core reactor, the optimized Fe-based soft magnetic reactor has a high voltage noise reduction of 31.9% and a sound power value

reduction of 28.7%. In addition, the background noise value also shows a decreasing trend, and the background noise of the optimized Fe-based soft magnetic reactor is 32.86 dB(A), which is 1.46 dB(A) lower than that of the silicon steel core reactor (34.32 dB(A)). The data indicate that the Fe-based soft magnetic composites based on the optimization algorithm can significantly suppress the noise radiation of the reactor, which verifies its potential for noise reduction in practical engineering.

Table 2: The audible noise of reactor samples dB (A)

	Background noise value (sound pressure value)	Measured noise value (high voltage value)	Measured noise value (sound power value)
Silicon steel core reactor	34.32	67.18	82.68
Magnetic powder core core reactor	33.56	50.47	65.25
The Fe-based soft magnetic composite reactor before optimization	33.18	47.42	62.31
The optimized Fe-based soft magnetic composite reactor	32.86	45.71	58.93

IV. Conclusion

In this study, the vibration noise mechanism and optimization control effect of Fe-based soft magnetic composite core reactor are systematically revealed through multi-physics field coupled simulation and experimental verification, and the main conclusions are as follows:

(1) The core vibration is mainly dominated by the Maxwell force, which causes the maximum displacement, 3.81×10^{-5}m, which is more than a thousand times of the magnetostrictive force, 3.56×10^{-8}m.

(2) Compared with the conventional silicon steel reactor, the vibration displacement of the Fe-based soft magnetic composite reactor is reduced by 98.61%, and the maximum displacement is reduced from 6.68×10^{-5}m to 9.41×10^{-7}m, which verifies the advantage of its low magnetostrictive property.

(3) Based on the electromagnetic-mechanical-acoustic coupling topology optimization algorithm, the vibration displacement of the Fe-based soft magnetic reactor is further reduced by 90.19%, which is 9.23×10^{-8}m after optimization), and the inductance value is only reduced by 4.98% from 4.22 mH to 4.01 mH, which significantly improves the damping effect under the premise of ensuring the performance.

(4) The optimized Fe-based soft magnetic reactor high-voltage noise is 45.71 dB(A), with the sound power value of 58.93 dB(A) compared with the silicon steel reactor were reduced by 31.9% and 28.7%, and the background noise is synchronously reduced to 32.86 dB(A), the noise reduction effect is significant.

Funding

This work was supported by State Grid Hebei Electric Power Co., Ltd. Science and technology project funding: A new type of low noise core reactor based on Fe-based soft magnetic composite material is developed (5204CZ240002).

References

[1] Callaway, D. S., & Hiskens, I. A. (2010). Achieving controllability of electric loads. Proceedings of the IEEE, 99(1), 184-199.
[2] Zhuikov, A. V., Matveev, D. A., Khrenov, S. I., & Nikulov, I. I. (2016). Minimization of high harmonics in the current of a biasing controlled arc suppressing reactor. Russian Electrical Engineering, 87, 439-445.
[3] Islam, M. M., Sutanto, D., & Muttaqi, K. M. (2019). Protecting PFC capacitors from overvoltage caused by harmonics and system resonance using high temperature superconducting reactors. IEEE Transactions on Applied Superconductivity, 29(2), 1-5.
[4] Li, S., Man, Y., Sun, Z., Li, S., Chen, R., & Zhao, C. (2020, December). A typical dry-type iron core reactor failure and its treatment measures. In IOP Conference Series: Earth and Environmental Science (Vol. 615, No. 1, p. 012067). IOP Publishing.
[5] Vashikar, V. V., & Prakash, S. (2022). Outrush Current Mitigation Using Iron Core Reactor. Special Education, 1(43).
[6] Zhang, Y., Zhu, L., Ji, S., Zhao, D., Zhang, X., & Li, Y. (2024, December). Research on Vibration Transmission Characteristics of Oil-immersed Iron-core Reactor based on Energy Power Flow. In 2024 4th International Conference on Smart Grid and Energy Internet (SGEI) (pp. 444-450). IEEE.
[7] Dimitrovski, A., Li, Z., & Ozpineci, B. (2014, April). Applications of saturable-core reactors (SCR) in power systems. In 2014 IEEE PES T&D Conference and Exposition (pp. 1-5). IEEE.
[8] Cazacu, E., & Petrescu, L. (2014, May). Magnetising inrush current of low-voltage iron core three phase power reactors. In 2014 16th International conference on harmonics and quality of power (ICHQP) (pp. 843-847). IEEE.
[9] Rosa, A. C. C. F. (2021). HV Sshunt Reactors: An Overall Comparative Analysis Between Dry-Type Air Core and Oil-Immersed Iron Core Technologies. Dissertação de Mestrado, UNIFEI-Universidade Federal de Itajubá.
[10] Ding, Z., Liu, L., & Liu, B. (2013). Modeling Analysis of DC Magnetic Bias of Iron Core Reactor of APF. Mathematical Problems in Engineering, 2013(1), 150129.

[11] Wu, P., Shi, Q., Shao, J., & Lu, Y. (2023, July). Study on Noise and Temperature Rise Characteristics of Iron-Based Soft Magnetic Composite-Silicon Steel Hybrid Core Reactor. In 2023 5th International Conference on Power and Energy Technology (ICPET) (pp. 810-813). IEEE.
[12] Li, J. Y., Liu, Z. J., Tang, B., Qin, R. S., Da Yu, Z., Liu, M. X., & Yang, G. L. (2022, September). Reactive Power Compensation Device Based on Magnetic-valve Controllable Reactor in the Treatment of Low Voltage at the End of Line. In 2022 7th International Conference on Power and Renewable Energy (ICPRE) (pp. 1-6). IEEE.
[13] Du, X., Tao, Y., Zheng, Y., Wang, C., Wang, Y., Qiu, S., ... & Zhai, Z. A. (2021). Reactor core design of UPR-s: a nuclear reactor for silence thermoelectric system NUSTER. Nuclear Engineering and Design, 383, 111404.
[14] Zhou, K., Li, Z., Gong, W., Zhao, S., Wen, C., & Song, Y. (2019). Influence of magnetic field generated by air core reactors in SVC-based substation and an optimal suppression method based on fuzzy comprehensive evaluation. IEEE Transactions on Electromagnetic Compatibility, 62(5), 1961-1970.
[15] Rathore, P., & Dommeti, V. (2020, October). Vibration and Noise Reduction Techniques of Gapped Core Shunt Reactor. In 2020 International Conference on Smart Technologies in Computing, Electrical and Electronics (ICSTCEE) (pp. 304-308). IEEE.
[16] Gao, Y., Nagata, M., Muramatsu, K., Fujiwara, K., Ishihara, Y., & Fukuchi, S. (2011). Noise reduction of a three-phase reactor by optimization of gaps between cores considering electromagnetism and magnetostriction. IEEE Transactions on Magnetics, 47(10), 2772-2775.
[17] Duc, H. B., Minh, T. P., Anh, T. P., & Quoc, V. D. (2022). A Novel Approach for the Modeling of Electromagnetic Forces in Air-Gap Shunt Reactors. Engineering, Technology & Applied Science Research, 12(1), 8223-8227.
[18] Yan, R., Gao, X., Zhu, L., Yang, Q., Ben, T., Li, Y., & Yang, W. (2016). Research on three-dimensional stress distribution of reactor core. IEEE Transactions on Applied Superconductivity, 26(4), 1-4.
[19] Zhang, P., Li, L., Cheng, Z., Tian, C., & Han, Y. (2018). Study on vibration of iron core of transformer and reactor based on maxwell stress and anisotropic magnetostriction. IEEE Transactions on Magnetics, 55(2), 1-5.
[20] Rossi, M., & Le Besnerais, J. (2015). Vibration reduction of inductors under magnetostrictive and Maxwell forces excitation. IEEE transactions on Magnetics, 51(12), 1-6.
[21] Rongge, Y., Weiying, L., Yuechao, W., Menghua, D., Xiaohong, Z., Lihua, Z., ... & Ying, S. (2017). Reactor vibration reduction based on giant magnetostrictive materials. AIP Advances, 7(5).
[22] Loizos, G., & Kladas, A. G. (2012). Core vibration analysis in Si-Fe distributed gap wound cores. IEEE transactions on magnetics, 48(4), 1617-1620.
[23] Wang, Z., Yu, R., Duan, C., Fan, Z., & Li, X. (2023, September). Analysis of the Vibration Characteristics and Vibration Reduction Methods of Iron Core Reactor. In Actuators (Vol. 12, No. 9, p. 365). MDPI.
[24] Zhu, S., Zhao, Y., & Shen, P. (2021, September). Optimal design of the dry-type iron core reactor based on the improved genetic algorithm. In 2021 8th International Forum on Electrical Engineering and Automation (IFEEA) (pp. 9-13). IEEE.
[25] Gao, L., Ji, S., Zhu, L., Yang, H., Zhang, F., Li, J., & Hui, S. (2021). Vibration and noise characteristics of air-core reactor used in HVDC converter stations. IEEE Transactions on Power Delivery, 37(2), 1068-1077.
[26] Adilbek, T., Irbulat, U., Yernar, A., & Dauirbek, A. (2024). Assessing noise and vibration mitigation in low-vibroacoustic shunt reactors. Cogent Engineering, 11(1), 2340325.
[27] Gao, Y., Muramatsu, K., Hatim, M. J., Fujiwara, K., Ishihara, Y., Fukuchi, S., & Takahata, T. (2010). Design of a reactor driven by inverter power supply to reduce the noise considering electromagnetism and magnetostriction. IEEE Transactions on Magnetics, 46(6), 2179-2182.
[28] Tong, B., Qingxin, Y., Rongge, Y., & Lihua, Z. (2017). Magnetically controlled saturable reactor core vibration under practical working conditions. IEEE Transactions on Magnetics, 53(6), 1-4.
[29] Moses, A. J., Anderson, P. I., & Phophongviwat, T. (2016). Localized surface vibration and acoustic noise emitted from laboratory-scale transformer cores assembled from grain-oriented electrical steel. IEEE Transactions on Magnetics, 52(10), 1-15.
[30] Verma, V., Chionis, D., Dokhane, A., & Ferroukhi, H. (2021). Studies of reactor noise response to vibrations of reactor internals and thermal-hydraulic fluctuations in PWRs. Annals of Nuclear Energy, 157, 108212.
[31] Huang, Q., Zhang, J., Fan, S., Zhang, Z., & Luo, C. (2020, November). Simulation analysis of vibration and noise characteristics of high voltage shunt reactor based on multi-physical field coupling. In IOP Conference Series: Earth and Environmental Science (Vol. 603, No. 1, p. 012044). IOP Publishing.